ELSEVIER

Journal of Nuclear Materials 266–269 (1999) 884–889

journal of nuclear materials

Radial and spectral profiles of atomic deuterium in front of a limiter in TEXTOR 94: Results of laser-induced fluorescence at Lyman-α

Ph. Mertens *, A. Pospieszczyk

Institut für Plasmaphysik, Forschungszentrum Jülich GmbH, EURATOM Association, Trilateral Euregio Cluster, D-52425 Jülich, Federal Republic of Germany

Abstract

Density profiles of atomic deuterium have been recorded in the plasma edge of TEXTOR 94, in front of a limiter, during ohmic discharges for central, line-averaged densities between 1.0×10^{19} and 3.0×10^{19} m^{-3}. The corresponding spectral profiles could be measured simultaneously for each radial position. They show, like previous measurements in the vicinity of the wall, the predominance of very slow atoms, below 1 eV (within the covered range of 0–10 eV kinetic energy in the radial direction). The profiles give indications about the presumed molecular origin of these slow atoms. © 1999 Elsevier Science B.V. All rights reserved.

Keywords: Atomic hydrogen; Deuterium; Laser-induced fluorescence; Velocity distribution; Plasma edge

1. Introduction

The role of the neutrals in the boundary layer of tokamaks comes gradually in a new light, as their importance is increasingly ascertained in connection with confinement properties [1,2], fueling [3], mode transitions [4,5], radiation cooling [6], helium exhaust and similar properties and effects which they may determine. One of the key issues to the characterization of recycling in this respect is the accurate identification of the mechanisms which are responsible for the release of hydrogen from plasma-facing components. These physical processes are not yet sufficiently understood for a complete description in the modeling codes, especially if one intends to use these codes for extrapolation to larger fusion devices. Such investigations are one of the main reasons for operating the laser-induced fluorescence (LIF) diagnostic in the vacuum-UV, usually at the Lyman-α transition of atomic deuterium.

The diagnostic system was originally described in [7] for the principles and in [8] as far as the implementation on TEXTOR is concerned. The density profiles of atomic deuterium recorded in front of the first wall (liner) for $r/a \approx 0.9$–1.2, together with the spectral profiles at different radial positions were discussed in [9,10]. This system was recently moved to another location on the torus: poloidally from the outboard, i.e. from the low-field side equatorial port, to the bottom and toroidally to the neighboring section; taking advantage of the existing limiter-lock to exchange components without breaking the vacuum of the tokamak vessel, it is now possible to measure density and velocity distribution of atomic hydrogen in the vicinity of standard limiters as well as at the wall [10]. The present paper brings in the first results of the measurements in front of graphite limiters.

2. Principles and experimental arrangement

As shown in the aforementioned publications, the third-harmonic radiation of a tunable, pulsed dye-laser with $E \geqslant 30$ mJ/pulse and about 200 W at $L_\alpha(\lambda_0 =$

* Corresponding author. Tel.: +49 2461 615720; fax: +49 2461 613331; e-mail: ph.mertens@fz-juelich.de.

0022-3115/99/$ – see front matter © 1999 Elsevier Science B.V. All rights reserved.
PII: S0022-3115(98)00616-3

121.534 nm) is sufficient to detect deuterium atoms in the ground state by LIF down to a density of about 8×10^{14} m^{-3} in the boundary layer of a middle-sized tokamak like TEXTOR 94. The spectral power density of the exciting radiation is nevertheless far below the saturation power of 3 MW/(cm^2 nm) at $L_\alpha(P \sim \lambda^{-5})$, to be compared with 0.2 kW distributed on about 1 cm^2 along with a laser spectral width of about 1 pm with étalon. The fluorescence radiation is thus proportional to the atomic density, to the cross-section for resonance fluorescence and to the vacuum-UV power available for excitation. The reasons why the Zeeman effect must not be taken into account for this scheme are explained in [9] and Ref. [16] therein; with a retardation plate inserted into the linearly polarized laser beam, only the π-components are excited. If the laser wavelength is scanned continuously during the plateau of the discharge, Doppler profiles are recorded, according to a wavelength shift of $\Delta\lambda = \lambda \times v/c$. It should be pointed out that the evaluation of the data is, for LIF, independent of the local plasma parameters like electron density or temperature.

The experimental set-up in the section of the limiter-lock is shown in Fig. 1. The frequency-tripling cell, filled with noble gases, is installed on top of the machine, directly at the entrance of the laser radiation into the tokamak. Three dielectric mirrors, optimized for the fundamental wavelength of $\lambda = 364.6$ nm and denoted as folding mirrors in the picture, are used in the light path between laser laboratory and focusing lens. They can be used for a rough alignment of the laser spot on the limiter head. The lens is motorized with a 2D-linear stage, in order to adjust the toroidal and poloidal position of the fluorescence volume remotely. Depending on the focusing into the gas cell, the diameter of the exciting beam lies around 10–14 mm, with a corresponding cross-section of 1.3 cm^2 at the observed radial position. With an extension of 5 mm in the radial direction, i.e. a spatial resolution of 5 mm perpendicular to the limiter surface at the present time, the fluorescence volume amounts to ≈0.7 cm^{-3}. It is usually positioned 20 mm away from the limiter tip in the toroidal direction, which – owing to the curvature of the limiter head – corresponds to a radial distance of 2.5 mm to the surface when limiter and observation volume both have the same nominal radius. Light reflection on the limiter is certainly much lower than in previous experiments in the near UV [11] since the surface is curved with a radius of 80 mm, the laser strikes it behind the apex and the rough graphite material is left without high polishing, but it cannot be ruled out completely. The fluorescence is observed at 90° with Cassegrainian optics, which can be tilted between tokamak shots to slide the measured point up and down, radially along the laser beam path.

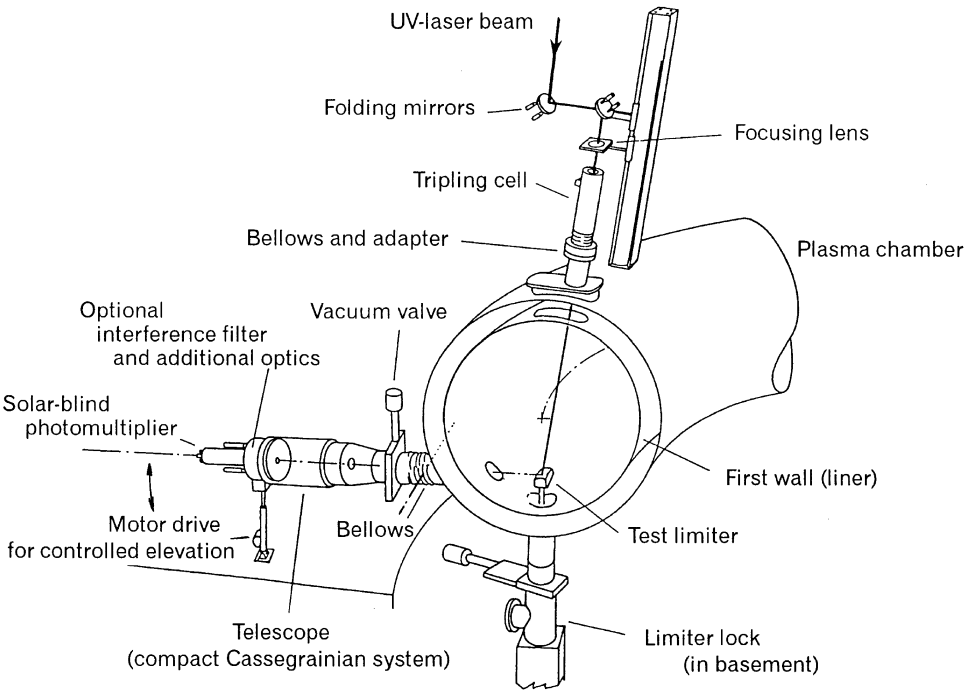

Fig. 1. Experimental set-up for the detection of atomic deuterium by laser-induced fluorescence in front of a limiter in TEXTOR 94 (the selective excitation takes place at Lyman-α). The observation telescope can be tilted with a step of 1 mm to move the fluorescence volume radially along the laser beam.

The spectral scan, with a resolution of 2.0–2.5 pm in the absence of Fabry–Perot, takes place within a single plasma discharge. The whole velocity distribution (at least for $E \approx 0$–20 eV) can thus be recorded by LIF with preservation of the spatial resolution. The solar-blind photomultiplier tube may be used with or without interference filter (transmission $T \approx 17\%$ at 120 nm); in any case, the observation system has no other spectral resolution than the rejection of distant wavelengths. The photomultiplier is pulsed with an adjustable gate width of 4–10 μs. It is connected to a digitizer of 500 MHz analog bandwidth and to a 'Boxcar' integrator, the integration width of which is set to 12 ns.

The present investigations took place in typical ohmic discharges at 2.0–2.5 T, a plasma current of 350 kA and a line-averaged central density of $\bar{n}_e = 1$–$3.0 \times 10^{19}\mathrm{m}^{-3}$. The measurements focused on atomic deuterium D^0 and the laser was operated at 20 Hz; with this repetition rate, the laser takes snapshots of about 5 ns duration. The main poloidal limiters or, alternatively, the toroidal belt limiter were positioned at the usual plasma radius of $r_{\mathrm{LIM}} = 460$ mm. Unless otherwise specified, the limiter head in the limiter-lock system was not heated actively, which means that its surface temperature did not exceed 1000 K in the standard case.

3. Results and discussion

The time evolution of the density of atomic deuterium was already documented in Ref. [9] as well as velocity distributions in front of the liner. A typical spectral profile as recorded a few millimeters in front of the limiter head is now shown in Fig. 2. It covers about 10 pm. It should be remembered though that (i) the conversion factor of the Doppler shift into velocities along the laser line amounts to about 250 km/s for 0.1 nm; (ii) in terms of energy, a velocity of about 1×10^4 m s^{-1}/4 pm can be scaled roughly to 1.0 eV for D^0; (iii) this possible conversion of the spectral shift into energies is valid for the velocity component in the direction of the laser beam only and accordingly does not reflect the kinetic energy of isotropically distributed particles: released atoms are likely to have a preferred propagation away from the surface they are ejected from. Since, for our geometrical configuration, the exciting radiation is impinging onto the surface of the plasma-facing material head-on from the top, a positive detuning $\Delta\lambda = \lambda - \lambda_0$, where λ_0 is the wavelength for deuterium atoms at rest, that is a detuning to the 'red' side, corresponds to atoms moving away from the limiter surface. *A contrario*, atoms on the 'blue' wing fly back to the limiter surface or leave the main plasma aiming at the first wall.

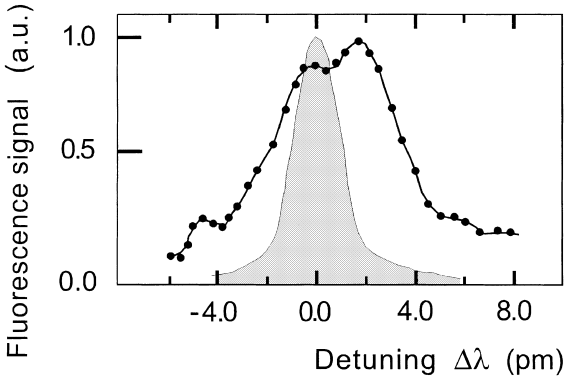

Fig. 2. Typical spectral profile recorded 5 mm in front of a graphite limiter head. In this example, each dot stands for two laser shots. The shaded curve represents the laser line at 121 nm.

The narrower profile depicted in Fig. 2 reproduces the laser spectral width as it can be extracted by deconvolution of the fluorescence signal from deuterium dissociated on a hot tungsten wire. Such atoms have a measured temperature of about 600 K, which results in a width of 1.44 pm when the laser is operated with étalon [7] to be compared with the expected thermal width of D^0, namely 1.25 pm when the fine structure is taken into account. Similarly for operation without étalon, the spectral profiles are scanned with the laser shown in the figure. The resolving power $\lambda/\Delta\lambda$ ranges from $R = 55{,}000$ (this work) to better than 150,000 with intracavity Fabry–Perot installed in the dye-laser.

Fig. 3 shows spectral profiles recorded while the limiter was gradually withdrawn from the radius of $r = 470$ mm (1 cm behind the last closed flux surface LCFS) to the position of the first wall (the liner has a radius of 546 mm). The curves are labeled with the radial position of the limiter surface and their amplitude is normalized for readability. A Savitsky–Golay algorithm was used for smoothing without influencing the form or width, which means that each dot represents about three laser shots. The fluorescence volume was kept at the radius of 470 mm. As a matter of fact, such measurements could not be performed with emission spectroscopy, owing to the unfavorable detection limit of the high-resolution arrangements; the S/N ratio would drop too rapidly with the removal of the surface. The top curve, at $r = 500$ should be compared with the profiles recorded at the wall in Ref. [9]. If the limiter is retracted, the profile is indeed representative for the situation at the wall. The curve stresses again the presence of neutral deuterium with very low energies, namely below 1 eV, at least in the scrape-off layer. The proposed explanations to their molecular origin were refined in the mean time for TEXTOR, in the light of the following contributions [12–14].

On the other hand for smaller radii, especially for 480 and 470 mm as shown in the two lower curves, the contribution of atoms which are leaving the surface to the plasma core is growing distinctly, with more than

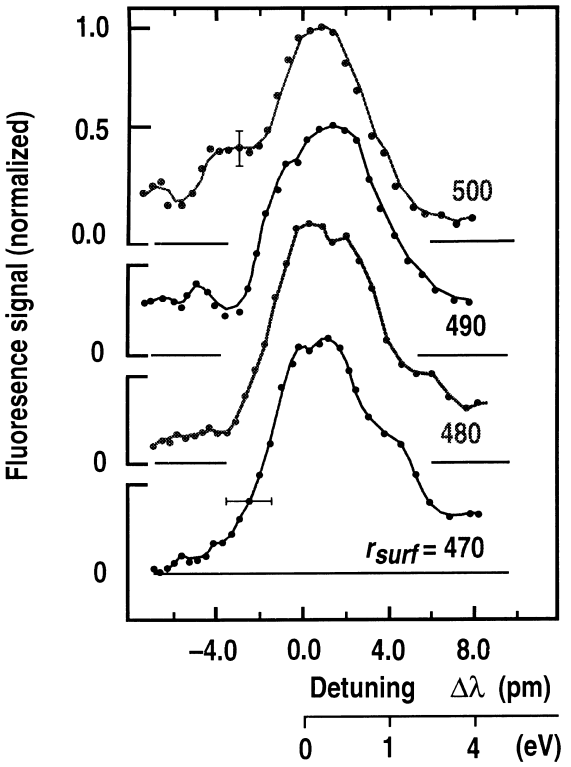

Fig. 3. Velocity distributions of atomic deuterium recorded just behind the LCFS. The observation volume is settled at 470 mm and the plasma-facing surface is progressively withdrawn – from the lower to the upper curve – until it can be assimilated to a wall element at $r = 500$ mm (shots 72190 sqq.).

25% of the peak value found between 6.0 and 8.0 pm, and probably somewhat higher if one extrapolates to higher detuning values (these could not be recorded while keeping the appropriate matching for the frequency conversion during the same plasma discharge but the assumption was verified afterwards, leading to a value of 28%). The corresponding velocities amount to $v_z \approx 2 \times 10^4$ m/s and more (4–10 eV range for the radial component of the velocity). This part of the profile is in agreement with earlier measurements of deuterium on carbon performed with high-resolution emission spectroscopy at the Balmer-α line in another toroidal sector, on another limiter specially prepared with observation dump [15]. It can be attributed for the largest part to the atoms which are reflected at the graphite surface with a most probable incidence angle to the normal around 50° as estimated by [16] and also to CX-neutrals which merge in this energy range [12]. Owing to the uncertainty in the determination of the reference wavelength, which is given by the error bar, a better quantitative evaluation of the profiles is not foreseen. For this purpose, a higher accuracy in the determination of λ_0 is required and a resolving power of $R \approx 100\,000$ is desirable.

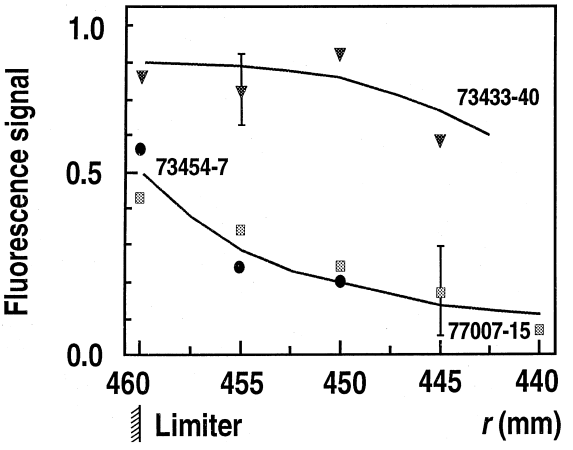

Fig. 4. Radial density profiles for low (▼ – $\bar{n}_e = 1.0$–1.5×10^{19} m^{-3}) and high (●, □ – $\bar{n}_e = 2.0$–3.0×10^{19} m^{-3}) line-averaged densities on axis. Ohmic shots with low surface temperature in the sense of [21], $B_T = 2.25$ T, $I_p = 350$ kA.

Radial density profiles are shown in Fig. 4 for standard ohmic discharges at low central density ($\bar{n}_e = 1.0$–1.5×10^{19} m^{-3} – upper curve) and at higher densities ($\bar{n}_e = 2.0$–3.0×10^{19} m^{-3} – lower curve, not accurately to scale with the former one). The radial profiles are rather flat, although a finer structure could give better clues to the location of the actual sources [14]. To avoid the profiles getting smeared, a reduction of the fluorescence volume from 5 to 3 mm radially seems to be experimentally within reach for the next campaign, without appreciable loss of spectral resolution. The first case, low line-averaged densities, matches the usual assumption of a penetration depth of several centimeters. Its estimation, with the velocity distribution recorded 5 mm inside the LCFS, amounts to 5 cm. The simple formula $\ell = \langle \bar{v} \rangle / \left(n_e \langle \sigma v \rangle_{ion} \right)$ gives, in spite of averaging the velocity twice – over the velocity distribution and over the radial stretch – and considering only electron-impact ionization, an estimation of 8 cm with $\langle \bar{v} \rangle = 5 \times 10^3$ m/s, with the local electron density and temperature $n_e(450) \approx 2 \times 10^{18}$ m^{-3} and $kT_e \approx 90$ eV [17], and $\langle \sigma v \rangle_{ion} = 3 \times 10^{-14}$ m^3/s.

The second case on the other hand (Fig. 4, lower points), corresponding to higher values for $\bar{n}_e$, which means for ohmic discharges in TEXTOR 94 $\bar{n}_e \approx 2.0$–4.0×10^{19} m^{-3}, shows a decay length which is considerably shorter than at low densities. The same rough estimation with the 'rule of thumb' formula recalled above gives $\ell = 4.6$ cm with $\langle \bar{v} \rangle = 4.5 \times 10^3$ m/s, with the local electron density $n_e(450) \approx 3.5 \times 10^{18}$ m^{-3}, $kT_e \approx 70$ eV, and $\langle \sigma v \rangle_{ion} = 2.8 \times 10^{-14}$ m^3/s, which seems to be too large by a factor of two (the radial kinetic energy of about 0.1 eV for the atoms should not be exceeded if the value of 2 cm is prescribed for ℓ). A better account of the contribution of $\langle \sigma v \rangle_{cx}$ may improve

this estimation for *slow* neutrals in the right direction. On the other hand, since the observed penetration depth is in agreement with H_α measurements [18] and since low kinetic energies are observed at each radial position separately in the interval shown, this is another indication of the presence of molecules with penetration depths of a few millimeters: an atomic source at the surface behaves differently, it leads to a spectral distribution which, from the beginning, shifts to higher velocities with increasing penetration, as a result of ionization of the slow component in the first place. One can compare this finding with the experimental results from molecular spectroscopy summarized in [18], keeping in mind the reservations conveyed in [19] with respect to the Fulcher bands.

In both cases shown in Fig. 4, the associated spectral distributions indeed stress the predominance of deuterium atoms in the spectral range 0.0–5.0 pm (0–1.6 eV) inside the LCFS (0–10 mm) as well. As has been said, this effect presumably reflects their molecular origin for a large part of the distribution (esp. $E \leqslant 1$ eV). The remaining contribution, especially around 1 eV, can possibly be compared with the surprisingly low energies of D^0-atoms released from hydrides by sputtering [20] or by the closely related ion-induced desorption (re-emission).

The suspected showing up of molecules is emphasized in the dependence of the fluorescence signal on the central density displayed in Fig. 5 (dots). Corroborating the finding that the contribution of molecules to the total hydrogen flux increases with $\bar{n}_e$ ([18], Fig. 13), the amplitude of the fluorescence signals at L_α decreases accordingly. The arrow heads $\Delta\lambda_{tot}$ give an impression of the decrease in the overall profile width which indicates a kind of 'cooling' due to the appearance of slow atoms originating in the molecules. But the deformation of the spectral distribution which takes place at the same time obviously restricts the applicability of a procedure which consists in defining such a profile width: contrary to a Gaussian spectral line centered on the reference wavelength, we consider a fine-structured velocity distribution which has nothing to do with the concept of temperature. A decrease of about 15% in the spectral linewidth may nevertheless be noticed but could not be fully asserted as long as the resolving power lies below 100,000. Similarly, heating of the limiter surface up to 1200 K causes a slight shift of the velocity distributions to longer wavelengths, indicating an increasing predominance of atomic against molecular release [18,21].

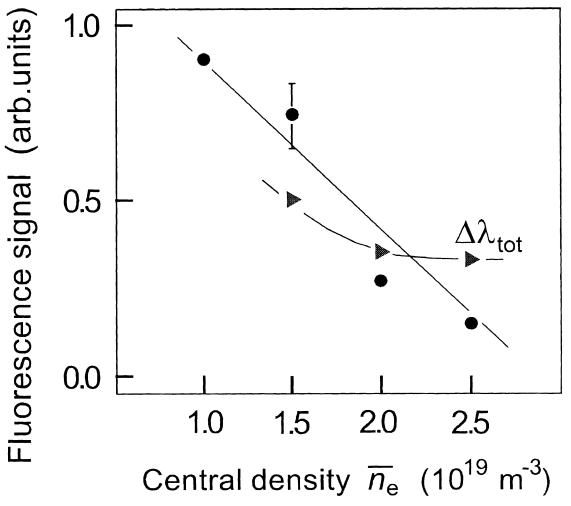

Fig. 5. Dependence of the atomic density (dots, recorded 7 mm away from the limiter surface) on the prescribed central density; the solid line is drawn to guide the eye. $\Delta\lambda_{tot}$ (pm) reflects the overall width of the spectral profiles and gives a very rough view of the energy of the observed atoms.

A quantitative explanation is still lacking for the high-density case. The following effects should be considered:

(a) we have clear indications for the stronger presence of molecules, which give rise to a substantial portion of the detected atoms. This happens under different mechanisms for molecular dissociation [14], in particular dissociative excitation as proposed in [9]. As far as the concommitant production of Balmer-α is concerned, [22] gave an estimated rate, which is discussed in [12]; possible dissociation channels have been picked out, which may account for the appearance of very low energies, down to 0.3 eV and simultaneously of higher ones, in the 6–17 eV range in contrast to the usual Franck–Condon atoms around 2.2 eV. This aspect is discussed in the present volume [18]. The apparent paradox is that higher electron temperatures may result, through collisional dissociation of molecules which are vibrationally excited, in lower kinetic energies of the dissociation products [14];
(b) we observe accordingly conditional velocity distributions, i.e. the velocity distribution of the atoms in the radial direction $f(v_{z,D^0})$ is a function of the velocity distribution of the molecules $f(v_{D_2},\ldots)$ [23], with which one has to consider the specific reactions mentioned here above for an isotropic dissociation;
(c) an integration into the modeling codes is desirable, the first step of which are documented in [18] in the case of EIRENE [24].

As far as the absolute density is concerned, no calibration with Rayleigh scattering could take place yet, for technical reasons. A hint to the actual values reached in the top curve of Fig. 4 is given by the flattening, or even the small notch in the spectral profiles recorded at high atomic densities as shown in Fig. 6. A similar behavior shows up with gas puff through the limiter head of a few times 10^{18} particles/discharge, i.e. within 5–10 s. It means a density n_{D^0} of about 5×10^{18} m^{-3} is attained

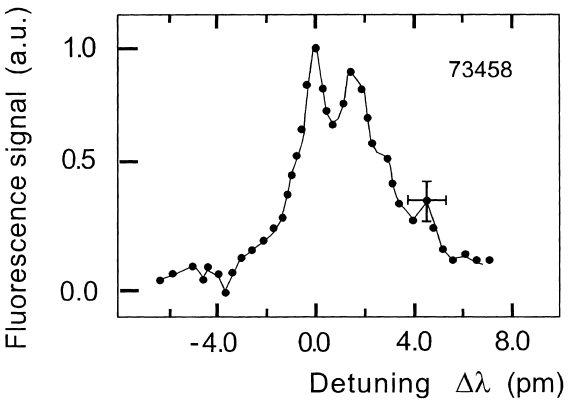

Fig. 6. Spectral profiles in the case of high atomic density $n_{D^0}(\bar{n}_e = 1.0 \times 10^{19}\ m^{-3}$; $B_T = 2.23$ T; $I_p = 360$ kA).

in front of the limiter, which corresponds to the limit where the Lyman-α line becomes optically thick for the velocities considered (cf. [25]). This will be checked later on, when an estimation of the density profiles is available in the poloidal direction of observation as well.

4. Conclusions and prospects

Laser-induced fluorescence in the vacuum-UV was used to record radial density profiles of atomic deuterium in front of plasma-facing components. It has been shown that the corresponding spectral profiles can be measured too, and that for each radial position in the range $r/a = 0.95$–1.2 (liner). These spectral profiles contain more information since they are a direct measure of the velocity distribution through the Doppler shift. A substantial contribution to the neutral density in the energy range 0–10 eV, up to 70%, has to be ascribed to slow atoms, below 1 eV (typically 0.3 eV radial kinetic energy), even for the radii observed inside the LCFS. The only explanation to their origin so far is that they were born from molecules along processes already discussed further in [9,12,14,18,22,23].

The measurements in front of a limiter are much more sensitive to a variation in the line-averaged central density (up to a factor of 2, depending on the radius) than the profiles recorded previously in the vicinity of the wall [9], where the increase with $\bar{n}_e$ was limited to 15%.

Although the accessibility was greatly reduced for the limiter region in comparison with the liner in the outer equatorial plane, this difficulty is partly compensated for by the higher atomic densities encountered, depending on the plasma parameters. An absolute value for this density is still lacking, but first estimations show that, under some conditions, the limit can be reached (just below $1 \times 10^{19}\ m^{-3}$) where the optical thickness of the Lyman-α line comes into play.

A better quantitative interpretation of the physical processes which were taken into account probably requires either an improved spatial, i.e. radial, resolution (a factor of two should be attainable fairly easily) or, preferably, an improved spectral resolution. This latter step may help in verifying to what extent parts of the distribution of the slow neutrals should be attributed to direct desorption. It still has to be made clear whether the possible improvement of the resolving power by a factor of three leaves enough energy per laser pulse for the actual detection limit.

References

[1] G.H. Wolf et al., in: J. Boedo (Ed.), Proc. 16th IAEA Fusion Energy Conf., vol. 1, 1997, pp. 177–185.
[2] A.M. Messiaen et al., Comments Plasma Phys. Controlled Fusion 18 (1997) 221.
[3] H. Takanega et al., J. Nucl. Mater. 241–243 (1997) 569.
[4] B.A. Carreras et al., Bull. Am. Phys. Soc. 41 (1996) 1573.
[5] A. Rogister, in: Ph. Mertens (Ed.), Proc. 3rd Workshop on Plasma and Laser Physics, Forschungszentrum Jülich GmbH, Bilat. Sem. Int., vol. 15, 1994, pp. 87–107, ISBN 3-89336-130-8.
[6] B. Unterberg et al., these Proceedings.
[7] Ph. Mertens, P. Bogen, Appl. Phys. A 43 (1987) 197.
[8] Ph. Mertens, P. Bogen, Proc. 16th Eur. Conf. on Controlled Fusion and Plasma Phys. vol. 13B, Part III, 1989, pp. 983–986.
[9] Ph. Mertens, M. Silz, J. Nucl. Mater. 241–243 (1997) 842.
[10] Ph. Mertens, in: A.J.H. Donné (Ed.), Proc. 8th Int. Symposium on Laser-Aided Plasma Diagnostics, LAPD-8, 1997, pp. 75–80.
[11] Ph. Mertens, P. Bogen, B. Schweer, Proc. 20th Eur. Conf. on Controlled Fusion and Plasma Phys. vol. 17C, Part III, 1993, pp. 1123–1126.
[12] J.D. Hey et al., Contrib. Plasma Phys. 36 (1996) 583–604.
[13] A. Pospieszczyk et al., Proc. 24th Eur. Conf. on Controlled Fusion and Plasma Phys. vol. 21A, Part IV, 1997, pp. 1733–1736.
[14] Ph. Mertens, Verhandl. DPG VI/33 (1998) 314 (German Phys. Soc. – in German).
[15] D. Reiter, P. Bogen, U. Samm, J. Nucl. Mater. 196–198 (1992) 1057.
[16] P. Lindner, private communication, 1998.
[17] B. Schweer, M. Brix, M. Lehnen, these Proceedings.
[18] A. Pospieszczyk et al., these Proceedings.
[19] U. Fantz et al., these Proceedings.
[20] Ph. Mertens, P. Bogen, J. Nucl. Mater. 128&129 (1984) 551–554.
[21] P. Franzen, E. Vietzke, J. Vac. Sci. Technol. A 12 (1994) 820.
[22] H. Tawara et al., J. Phys. Chem. Ref. Data 19/3 (1990) 617.
[23] P.Th. Greenland, private communication.
[24] D. Reiter, in: R.K. Janev, H.W. Drawin (Eds.), Atomic and Plasma–Material Interaction Processes in Controlled Thermonuclear Fusion, Elsevier, 1993, pp. 243–266.
[25] K. Behringer, MPI Plasmaphys., Garching, Report IPP 10-5, 1997, 21 pp.